New alleles of *D-2-hydroxyglutarate dehydrogenase* enable studies of oncometabolite function in *Drosophila melanogaster*

Madhulika Rai[1], Prince Okah[1§], Shefali A. Shefali[1§], Alexander J. Fitt[1§], Michael Z. Shen[1§], Mandkhai Molomjamts[1], Robert Pepin[2], Travis Nemkov[3], Angelo D'Alessandro[3], and Jason M. Tennessen[1,4*]

[1]Department of Biology, Indiana University, Bloomington, IN 47405, USA
[2]Department of Chemistry, Indiana University, Bloomington, IN 47405, USA
[3]Department of Biochemistry and Molecular Genetics, University of Colorado Anschutz Medical Campus, Colorado, USA
[4]Affiliate Member, Melvin and Bren Simon Cancer Center, Indianapolis, IN, 46202, USA

*Corresponding author; email: jtenness@iu.edu
[§]These authors contributed equally to the study.

Key words: *Drosophila melanogaster*, metabolism, D-2HG, oncometabolite, d-2-hydroxyglutarate dehydrogenase, D2hgdh

ABSTRACT

D-2-hydroxyglutarate (D-2HG) is a potent oncometabolite capable of disrupting chromatin architecture, altering metabolism, and promoting cellular dedifferentiation. As a result, ectopic D-2HG accumulation induces neurometabolic disorders and promotes progression of multiple cancers. However, the disease-associated effects of ectopic D-2HG accumulation are dependent on genetic context. Specifically, neomorphic mutations in the mammalian genes *Isocitrate dehydrogenase 1* (*IDH1*) and *IDH2* result in the production of enzymes that inappropriately generate D-2HG from α-ketoglutarate (αKG). Within this genetic background, D-2HG acts as an oncometabolite and is associated with multiple cancers, including several diffuse gliomas. In contrast, loss-of-function mutations in the gene *D-2-hydroxyglutarate dehydrogenase* (D2hgdh) render cells unable to degrade D-2HG, resulting in excessive buildup of this molecule. *D2hgdh* mutations, however, are not generally associated with elevated cancer risk. This discrepancy raises the question as to why ectopic D-2HG accumulation in humans induces context-dependent disease outcomes. To enable such genetic studies *in vivo*, we generated two novel loss-of-function mutations in the *Drosophila melanogaster* gene *D2hgdh* and validated that these alleles result in ectopic D-2HG. Moreover, we observed that *D2hgdh* mutations induce developmental and metabolomic phenotypes indicative of elevated D-2HG accumulation. Overall, our efforts provide the *Drosophila* community with new mutant strains that can be used to study D-2HG function in human disease models as well as in the context of normal growth, metabolism, and physiology.

INTRODUCTION

D-2-hydroxyglutarate (D-2HG) is a tricarboxylic acid produced from the citric acid cycle intermediate alpha-ketoglutarate (αKG) (YE *et al.* 2018; DU AND HU 2021). Under physiological conditions, animals can synthesize D-2HG by two enzymatic mechanisms: (i) the enzyme Hydroxyacid-Oxoacid Transhydrogenase (HOT) interconverts αKG and γ-hydroxybutyrate into succinic semialdehyde and D-2HG (STRUYS *et al.* 2005b); and (ii) the noncanonical activity of the enzyme d-3-phosphoglycerate dehydrogenase reduces αKG to form D-2HG (FAN *et al.* 2015). However, despite being an intermediate metabolite in normal cellular metabolism, intracellular D-2HG concentration remain relatively low due, in part, to the activity of the mitochondrial enzyme D-2-hydroxyglutarate dehydrogenase (D2HGDH), which converts D-2HG into αKG in an FAD dependent manner (ACHOURI *et al.* 2004).

The D2hgdh-imposed limitation on D-2HG pool size is essential for normal cellular function, as D-2HG is a potent signaling molecule capable of inhibiting a wide-range of αKG-dependent dioxygenases, including the Jmj class of histone lysine demethylases, the Tet family of enzymes, and prolyl hydroxylases (FIGUEROA *et al.* 2010; CHOWDHURY *et al.* 2011). As a result, increased D-2HG accumulation can induce dramatic changes in chromatin architecture, gene expression, and cellular metabolism, and ultimately lead to a variety of disease phenotypes (YE *et al.* 2018; DU AND HU 2021). For example, loss-of-function mutations in the human *D2hgdh* gene result in an inborn error of metabolism known as D-2-hydroxyglutaric aciduria, which is characterized by elevated urinary D-2HG levels, developmental delays, seizures, and brain abnormalities (STRUYS *et al.* 2005a; STRUYS 2006).

Due to the manner by which D-2HG interferes with αKG-dependent processes, this molecule is also capable of acting as an oncometabolite and is well-documented to promote the

growth and development of a wide range of tumors (YE *et al.* 2018; WANG *et al.* 2020; CHOU *et al.* 2021; DU AND HU 2021). The associations between D-2HG and cancer, however, are sensitive to the mechanism that induces excess D-2HG accumulation. In nearly all documented studies of tumors that accumulate D-2HG, the underlying cause is a neomorphic mutation in either *IDH1* or *IDH2* (DANG *et al.* 2009; LOSMAN AND KAELIN 2013). These mutations alter the catalytic activity of IDH1/2 in a manner that induces inappropriate D-2HG production (LOSMAN AND KAELIN 2013). Such mutations are found in wide variety of tumors and are exceedingly common in certain gliomas, with, 70%-80% of grade II and III astrocytomas harboring *Idh1* mutations (YANG *et al.* 2020). In fact, the widespread occurrence of *IDH1* mutations in gliomas and acute myeloid leukemia has led to the successful development of FDA approved IDH inhibitors (GATTO *et al.* 2021; TIAN *et al.* 2022), which are now used in combination therapies to treat Idh positive tumors.

While there is overwhelming evidence that D-2HG acts as an oncometabolite in cells that express mutant IDH1/2, only a handful of studies link *D2hgdh* mutations with increased cancer risk (ADAM *et al.* 2021) – a striking observation considering that IDH1/2 mutations are present in a majority of grade II and III astrocytomas. This observation raises the question as to why D-2HG only acts as an oncometabolite in specific genetic backgrounds and highlights the need to further study endogenous D-2HG metabolism in both healthy tissues and disease models. Towards this goal, we are using the fruit fly *Drosophila melanogaster* as a model to understand how loss of D2hgdh activity affects metabolism, growth, and development.

Similar to humans and mice, *Drosophila* relies on D2hgdh to limit D-2HG accumulation, as D-2HG levels are relatively low throughout the fly lifecycle and RNAi depletion of *Drosophila D2hgdh* expression results in elevated 2HG accumulation (REITMAN *et al.* 2015; LI

115 *et al.* 2017; MAHMOUDZADEH *et al.* 2020). Moreover, flies expressing an oncogenic *Idh* mutant
116 allele accumulate elevated 2HG levels and produce excess blood cells (hemocytes) (REITMAN *et*
117 *al.* 2015), thus indicating that expression of neomorphic Idh variants in flies partially
118 phenocopies the cancer associated Idh1/2 phenotypes. These earlier studies, however, largely
119 ignored the endogenous biological functions of D-2HG and D2hgdh and were instead focused on
120 the oncogenic effects of mutant Idh expression. We would also note that while several studies
121 focusing on L-2HG have also examined D-2HG levels (LI *et al.* 2017; LI *et al.* 2018;
122 MAHMOUDZADEH *et al.* 2020), these investigations did not examine the role of D-2HG in
123 development, physiology, or metabolism.

124 In order to facilitate additional studies of D-2HG metabolism in *Drosophila*, we used a
125 CRISPR/Cas9 approach to generate loss-of-function mutations in *D2hgdh*. Here we demonstrate
126 that the resulting mutant lines are viable and display elevated D-2HG levels. Moreover, *D2hgdh*
127 mutants exhibit decreased fecundity and viability, as well as occasional formation of melanotic
128 masses, which is often indicative of altered immune signaling. Finally, metabolomic analysis of
129 adult male *D2hgdh* mutants reveal significant changes in essential amino acids levels. Overall,
130 our findings establish *Drosophila* as a powerful genetic model for studying endogenous D-2HG
131 metabolism and suggest that future studies of the *D2hgdh* mutants will advance our
132 understanding of how loss of D2hgdh activity results in disease phenotypes.
133

MATERIALS AND METHODS

Drosophila melanogaster husbandry

Fly stocks were maintained at 25°C on Bloomington Drosophila Stock Center (BDSC) food. Larvae were raised on molasses agar plates with yeast paste spread over the surface as previously described (LI AND TENNESSEN 2017). All mutations were studied in a w^{1118} background. For all adult analysis, males and virgin females were collected within 8 hours of eclosion, the sexes separated into vials containing BDSC food, and animals were aged for 5-7 days. Flies were then anesthetized using carbon dioxide and collected immediately for subsequent analysis. Flybase was used as an essential reference tool throughout this study (GRAMATES *et al.* 2022; ÖZTÜRK-ÇOLAK *et al.* 2024).

Generation of *D2hgdh* mutations

D2hgdh mutations were generated using CRISPR/Cas9 (GRATZ *et al.* 2013; SEBO *et al.* 2014). An oligo encoding a guide RNA sequence that targeted exon 3 of the *D2hgdh* locus (5’ CTTCGCTTAAGCCCGGAAGCACGG 3’) was inserted into the BbsI site of pU6-BbSI-gRNA (Addgene). The gRNA construct was injected into RRID:BDSC_51324 (w[1118]; PBac{y[+mDint2]=vas-Cas9}VK00027). Two mutations isolated from independently injected embryos were identified by PCR amplification of the region surrounding exon 2 of the *D2hgdh* locus using oligos 5’- TCCTCCACGATGAGATTCCAAC -3’ and 5’- TGATCGAAGTTCTCCAGGATGC -3’. The resulting PCR product was sequenced using oligos 5’- CCTATCACCACCACCACCATC-3’ and 5’- AAGGACAATCTCGTCGCAGATC-3’. This approach identified two *D2hgdh* deletions: $D2hghd^{12\text{-}6}$ consists of a 76 bp deletion (5’- CCACTCTGACCGACAAGGATGTGGCGCATTTCGAGCAGCTCCTGGGCAAGAACTTC

157 GTGCTCACTGAGGACCTGGA-3'). *D2hghd*$^{5-5}$ contains a 5 bp deletion of 5'-GACCT-3'
158 within the sequence 5'-GAACTTCGTGCTCACTGAGGACCTGG-3' (see Figure 1A).
159
160 **Gas Chromatography-Mass Spectrometry (GC-MS) analysis**
161 D- and L-2HG were quantified using a protocol specifically designed for analyzing these
162 two metabolites (LI AND TENNESSEN 2019). Briefly, either 25 mid-L2 larvae or 20 adults (5-7
163 days post-eclosion) were placed in a pre-tared 2 ml screw cap tube containing 1.4 mm ceramic
164 beads (Catalog No. 15-340-153; Fisher Scientific), the mass was determined with an analytical
165 balance, and the tube was immediately dropped into liquid nitrogen and subsequently stored at -
166 80°C until processing. 800 µl of ice cold extraction buffer (90% MeOH with 8 mg of 2,2,3-d3-
167 R,S-2-hydroxyglutarate) was then added to each sample (kept in -20ºC enzyme caddies) and
168 tubes were then immediately placed in a Omni Bead Ruptor 24 and homogenized for 30 seconds
169 at 6.4 m/s. Samples were subsequently incubated at -20ºC for 1 hr. After the incubation, samples
170 were centrifuged at 20,000 x g for 5 min at 4ºC. 600 µl of the supernatant was then transferred
171 into a 1.5 mL microfuge tube and dried overnight using a vacuum centrifuge.
172 Dried samples were resuspended in 50 µl of R-2-Butanol and 5 µl of HCL and incubated
173 at 90ºC for three hours with shaking at 300 rpm using an Eppendorf ThermoMixer F1.5. After
174 cooling, 200 µl of water and 500 µl of hexane was added to each tube. The organic phase
175 (hexane) was then transferred to a new tube and dried for 30 minutes using a vacuum centrifuge.
176 The dried samples were resuspended in 60 µl of acetic anhydride and 60 µl of pyridine and
177 incubated at 80ºC for 1 hr with shaking at 300 rpm. Samples were then dried for 3 hrs using a
178 vacuum centrifuge and resuspended in 60 µl of hexane. GC-MS analyses were performed using

an Agilent GC6890-5973i MS equipped with a Gerstel MPS autosampler and a 30 m Phenomex ZB5-5 MSi column.

Ultra High-pressure Liquid Chromatography - Mass Spectrometry (UHPLC-MS)-based Metabolomics

D2hgdh mutants and the control strain were raised on BDSC food at 25ºC and groups of 20 newly eclosed adult males were transferred to a fresh vial and aged for 5 days, at which point they were placed in a 1.5 mL microfuge tube and drop frozen in liquid nitrogen. Samples were then individually transferred to a pretared 1.4 mm bead tube, the mass was measured using a Mettler Toledo XS105 balance, and the sample was returned to a liquid nitrogen bath prior to being stored at -80°C. Samples were subsequently homogenized in 0.8 mL of prechilled (-20 °C) 90% methanol containing 2 µg/mL succinic-d4 acid, for 30 seconds at 6.45 m/s using a bead mill homogenizer located in a 4°C temperature control room. The homogenized samples were incubated at -20 °C for 1 hour and then centrifuged at 20,000 × g for 5 min at 4°C. The resulting supernatant was sent for metabolomics analysis at the University of Colorado Anschutz Medical Campus, as previously described (Nemkov et al., 2019).

UHPLC-MS metabolomics analyses were performed at the University of Colorado Anschutz Medical Campus, as previously described (NEMKOV *et al.* 2019). Briefly, the analytical platform employs a Vanquish UHPLC system (Thermo Fisher Scientific, San Jose, CA, USA) coupled online to a Q Exactive mass spectrometer (Thermo Fisher Scientific, San Jose, CA, USA). The (semi)polar extracts were resolved over a Kinetex C18 column, 2.1 x 150 mm, 1.7 µm particle size (Phenomenex, Torrance, CA, USA) equipped with a guard column (SecurityGuard™ Ultracartridge – UHPLC C18 for 2.1 mm ID Columns – AJO-8782 –

Phenomenex, Torrance, CA, USA) using an aqueous phase (A) of water and 0.1% formic acid and a mobile phase (B) of acetonitrile and 0.1% formic acid for positive ion polarity mode, and an aqueous phase (A) of water:acetonitrile (95:5) with 1 mM ammonium acetate and a mobile phase (B) of acetonitrile:water (95:5) with 1 mM ammonium acetate for negative ion polarity mode. The Q Exactive mass spectrometer (Thermo Fisher Scientific, San Jose, CA, USA) was operated independently in positive or negative ion mode, scanning in Full MS mode (2 μscans) from 60 to 900 m/z at 70,000 resolution, with 4 kV spray voltage, 45 sheath gas, 15 auxiliary gas. Calibration was performed prior to analysis using the Pierce™ Positive and Negative Ion Calibration Solutions (Thermo Fisher Scientific).

Statistical Analysis of Metabolomics Data

Both metabolomics datasets were analyzed using Metaboanalyst 5.0 (PANG *et al.* 2021). Samples were normalized to mass and the data was preprocessed using log normalization and Pareto scaling. Preprocessed data can be found in Table S1.

Characterization of Developmental Phenotypes

Twenty-five males and 50 virgin females for the control and mutant genotypes were placed in an egg laying chamber and placed in a 25ºC incubator. For fecundity assays, flies were mated for 24 hours prior to start of the assay, after which egg-laying plates were placed in the chamber for one-hour intervals and the number of eggs were counted by visual observation in using a standard dissection microscope. Embryonic viability was measured by counting the number of eggs on each egg-laying plate that hatched 24 hrs after egg-laying. Larval length was determined 5 days after egg-laying. Pupal viability was measured by transferring 20 newly

hatched L1 larvae to a food vial and subsequently counting the number of pupae until 8 days after egg-laying.

Statistical Analysis

All data analyses were conducted using Graphpad Prism 9. All samples were analyzed using an ANOVA test followed by a Tukey's multiple comparison test.

RESULTS

D2hgdh mutants accumulate excess D-2HG

As a first step towards determining how D2hgdh activity regulates D-2HG levels during the *Drosophila* life-cycle, we used CRISPR/Cas9 to generate two mutations in the *D2hgdh* gene. As described in the methods, our approach isolated two *D2hgdh* mutant alleles consisting of a 5 bp deletion ($D2hgdh^{5\text{-}5}$) and a 76 bp deletion ($D2hghd^{12\text{-}6}$), both of which disrupt the conserved catalytic region of the enzyme (Figure 1A; see Methods for a description of the deleted regions). The resulting mutants are homozygous/hemizygous viable, thus allowing us to determine if *D2hgdh* mutations alter steady state D-2HG levels at multiple points during the life-cycle. Consistent with the conserved role of D2hgdh in catabolizing D-2HG, both $D2hgdh^{5\text{-}5}$ and $D2hghd^{12\text{-}6}$ mutant males, females, and L2 larvae displayed significantly higher D-2HG levels as compared with controls (Figure 1B-D). In contrast, L-2HG levels were either unchanged or decreased in *D2hgdh* mutants, indicating that D2hgdh activity is specific to D-2HG (Figure 1E-G). These results demonstrate that *D2hgdh* encodes the enzyme responsible for limiting D-2HG accumulation in the fly.

D2hgdh mutants develop melanotic masses and display developmental defects

D2hgdh mutations in humans lead to developmental delays and as well as hypermelanization of the abdominal region, a condition termed angiokeratoma, which is represent benign lesions on the skin (PRESTON *et al*. 2019). Consistent with these human disease phenotypes, we observe similar phenomenon in *D2hgdh* mutants - both $D2hgdh^{5\text{-}5}$ and $D2hghd^{12\text{-}6}$ mutant larvae exhibit melanotic masses within their abdominal cavity (Figure 2A-C). While these lesions are relatively rare (present in ~2% of larvae; Figure 2C), the masses are easily

observed and occur at similar rates in both strains. Moreover, a closer examination of the lesions using confocal microscopy reveal that these masses were often associated with regions of the hindgut that lacked nuclei (Figure 2D-I). While we are unsure of the significance of these lesions, we would note that a similar observation was made in larvae that express the *UAS-Idh*^{mut} transgene that induces ectopic D-2HG formation (REITMAN *et al.* 2015), suggesting that the masses likely result from elevated D-2HG levels.

In addition to the melanotic mass phenotype, *D2hgdh* mutants also exhibit developmental defects. We notably observed that both *D2hgdh*$^{5-5}$ and *D2hghd*$^{12-6}$ mutant females exhibit reduced fecundity when compared with *w*^{1118} controls (Figure 3A). Moreover, we also observed a significant reduction in the viability of those eggs laid by *D2hgdh*$^{5-5}$ and *D2hghd*$^{12-6}$ mutants (Figure 3B). However, we observed no decrease in either larval or pupal viability (Figure 3C,D), thus indicating that D2hgdh isn't absolutely required for viability.

Metabolomics analysis of *D2hgdh* mutants

To better understand how loss of D2hgdh activity alters *Drosophila* metabolism and physiology, we used a metabolomics approach to compare adult male *D2hgdh*$^{5-5}$ and *D2hghd*$^{12-6}$ mutants with *w*^{1118} controls. Principle component analysis of the resulting datasets revealed that the metabolomic profiles of both mutant strains significantly differ from the control strain but not from each other, demonstrating that loss of D2hgdh activity appreciably alters the metabolome of adult male flies (Figure 4A). Moreover, both mutant strains exhibit similar changes in metabolite abundance (Figure 4B), suggesting that metabolic phenotypes observed in these are not the result of genetic background effects.

Overall, the metabolomic profile of *D2hgdh* mutants highlight disruptions of carbohydrate and amino acid metabolism. Both mutant strains exhibit elevated levels of a hexose-phosphate as well as erythrose-4-phosphate, an intermediate in the pentose phosphate pathway, as well as the nucleotides ITP and CTP as UMP and cGMP (Figure 4B). In contrast, we observed decreased levels of the purine degradation products xanthine and hypoxanthine, perhaps suggesting that D-2HG influences purine metabolism. We also observed a highly significant decrease in cadaverine – a breakdown product of lysine commonly found in bacteria. Similarly, N6-N6-N6-trimethyl-L-lysine levels were also significantly lower in mutant males when compared with adults.

Finally, two metabolites failed to produce the expected changes in *D2hgdh* mutants. First, 2HG levels were not significantly altered in our analysis (Table S1; Figure 4C). We would note, however, that the semi-targeted analysis used for this study does not differentiate between D-2HG and L-2HG, and thus the observed 2HG values represents the relative abundance of both molecules. As noted above, *D2hgdh* mutant male flies tend to harbor normal levels of L-2HG (See Figure 1), which would partially mask any increase in D-2HG. We also failed to observe an increase in lysine levels, which differs from a recent metabolomic studies of *C. elegans*, where *dhgd-1* mutants displayed increased lysine accumulation (PONOMAROVA *et al.* 2023). In fact, we observed the opposite phenomenon, as lysine was slightly downregulated in one mutant strain as compared with controls (Figure 4C). This result might indicate that *Drosophila* D2hgdh activity influences certain aspects of cellular metabolism in manner that is distinct from that of the *C. elegans* D2hgdh homolog.

DISCUSSION

Here we establish a new genetic model for studying the role of D2hgdh in animal metabolism, physiology, and development. Our studies demonstrate that D2hgdh is the key enzyme responsible for regulating D-2HG levels in the fly, as loss of this enzyme in larvae, adult males, and adult females results in a significant increase in D-2HG levels when compared with a control strain. Moreover, we find that *D2hgdh* mutants display reduced fecundity and a larval growth phenotype. Finally, metabolomics analysis of these mutants reveals significant changes in the abundance of carbohydrates, nucleotides, and lysine catabolic products. Overall, our studies demonstrate that these *D2hgdh* novel mutations produce a subset of phenotypes consistent with those observed in human D-2-HG aciduria patients and are appropriate for studying D-2HG within the context of human disease models.

While previous studies in the fly examined the effects of ectopic D-2HG production by driving expression of a *UAS-Idh*^{mut} transgene (REITMAN *et al*. 2015), our study is the first to examine the phenotypic consequences of mutating *D2hgdh*. Interestingly, we find that our *Drosophila D2hgdh* mutants display some phenotypes in common with flies expressing the *UAS-Idh*^{mut} transgene. In this regard, both the occasional presence of melanotic masses within *D2hgdh* mutant larvae and the metabolomics profile of adult *D2hgdh* mutant males are notable. The presence of melanotic masses within *D2hgdh* larvae raises several interesting questions about the nature of this phenotype and similarities with human patients. As mentioned above, the human inborn error of metabolism is associated with hypermelanization of the abdominal region (PRESTON *et al*. 2019). While the cause of this phenomenon remains unknown, our observations in the *D2hgdh* mutant, combined with a previous study describing melanotic masses in flies

328 expressing the *UAS-Idh*^{mut} transgene, suggest that a conserved metabolic mechanism links
329 elevated D-2HG metabolism with this poorly understood phenomenon.

330 One interesting, albeit speculative, possibility is that the hypermelanization phenotype
331 displayed by *D2hgdh* mutants is that it results from altered immune cell activity – a hypothesis
332 supported by several observations. First, overexpression of the *UAS-Idh*^{mut} transgene induces
333 increased levels of hemocytes, demonstrating that D-2HG induces increased levels of immune
334 cells within flies (REITMAN *et al.* 2015). Secondly, excess D-2HG accumulation alters CD8 T
335 lymphocyte activity and *D2hgdh* knockdown decreased the anti-tumor activity of these cells
336 (YANG *et al.* 2022). Future studies should determine if *D2hgdh* mutant larvae display changes in
337 immune cell numbers and/or an altered immune response.

338 Finally, the metabolomics profile of *D2hgdh* mutants display several unexpected
339 changes, with two trends being of particular interest. First, we observed significant changes in
340 nucleotide metabolism – several nucleotides were significantly upregulated in both mutant
341 background while xanthine and hypoxanthine, products of purine catabolism, are decreased. We
342 are uncertain as to the significance of these findings, however, the results hint at a role for D-
343 2HG in regulating nucleic acid metabolism. The second important observation is that lysine does
344 not accumulate in *D2hgdh* mutants. We expected to observe elevated lysine because (i) the
345 enzyme that degrades lysine is inhibited by D-2HG (CHOWDHURY *et al.* 2011), (ii) *C. elegans*
346 *dhgd-1* mutants accumulate lysine (PONOMAROVA *et al.* 2023), and (iii) *L2hgdh* mutants exhibit
347 elevated lysine levels (MAHMOUDZADEH *et al.* 2024). Considering that lysine is either unchanged
348 or decreased in *Drosophila* mutants, this result suggests that the relationship between D-2HG
349 and lysine metabolism is more complex than previously anticipated. We would also note lysine

is unchanged in D2HG aciduria patients (GIBSON *et al.* 1993; KRANENDIJK *et al.* 2012), thus highlighting a need to further examine this metabolic interaction.

ACKNOWLEDGEMENTS

We thank the Bloomington *Drosophila* Stock Center (NIH P40OD018537) for providing fly stocks, the *Drosophila* Genomics Resource Center (NIH 2P40OD010949) for genomic reagents, and Flybase (NIH 5U41HG000739). GC-MS was conducted using instruments housed in the Indiana University Mass Spectrometry Facility. A.J.F. was supported by the Indiana University Cox Scholars Program. SS was supported by the John R. and Wendy L. Kindig Fellowship, Briggs Fellowship, Dona Graam Fellowship through Indiana University, and an American Heart Association Predoctoral Fellowship (25PRE1372770). J.M.T. is supported by the National Institute of General Medical Sciences of the National Institutes of Health under a R35 Maximizing Investigators' Research Award (MIRA; 1R35GM119557).

DATA AVAILABILITY

The w^{1118} *D2hgdh*$^{5-5}$ and w^{1118} *D2hghd*$^{12-6}$ strains have been deposited in the Bloomington *Drosophila* Stock Center and are also available upon request. Metabolomics data is present within Table S1.

FIGURE LEGENDS

Figure 1. *D2hgdh* mutations induce elevated D-2HG accumulation. (A) A schematic diagram illustrating the *D2hgdh* locus and the mutations $D2hgdh^{12\text{-}6}$ and $D2hgdh^{5\text{-}5}$. The arrow under Δ5-5 points to the location of the $D2hgdh^{5\text{-}5}$ 7 bp deletion. The bracket next to Δ12-6 illustrates to the location of the $D2hgdh^{5\text{-}5}$ 76 bp deletion. (B-G) The amount of D-2HG and L-2HG were simultaneously quantified in both control and *D2hgdh* mutants during the (B,E) L2 larval stage as well as in (C,F) adult males and (D,G) adult females. Data presented as a scatter plot with the lines representing the mean and standard deviation. *P*-values calculated using a Wilcoxon/Kruskal-Wallis tests followed by a Dunn's test to compare mutant sample with control. **P*<0.05. ***P*<0.01. ****P*<0.001.

Figure 2. *D2hgdh* mutant exhibt melanotic mass formation. Unlike (A) w^{1118} controls, (B) *D2hgdh* mutant develop melanotic masses in their abdominal region. (C) The melanotic mass phenotype occurs in ~2% of larvae. Data presented as a scatter plot with the lines representing the mean and standard deviation. (D-I) Larval intestine from w^{1118} controls and *D2hgdh* mutants with melanotic masses were dissected and stained with DAPI. (E,F) These lesions are most prevalent in the mutant hindgut and (H,I) are associated with regions that lack of DAPI stained nuclei. (H,I) Red arrows point to melanotic masses in confocal images. The scale bar representing 200 μM in (D) applies to (E,F). The scale bar representing 200 μM in (G) applies to (H,I).

Figure 3. *D2hgdh* mutants exhibit several developmental phenotypes. When compared with the w^{1118} control strain, both $D2hgdh^{12\text{-}6}$ and $D2hgdh^{5\text{-}5}$ mutants exhibit significant decreases in (A) fecundity and (B) embryonic viability. In contrast, both (C) pupation rate at 8 days after egg-laying (D8AEL) and (D) eclosion rate were similar across all three strains. Data are presented in scatter plots with mean ± standard deviation. *P*-values calculated using a Wilcoxon/Kruskal-Wallis tests followed by a Dunn's test to compare mutant sample with control. **P*<0.05. ***P*<0.01. ****P*<0.001. Note that all *P*-values compare the indicated mutant samples with the control.

Figure 4. Targeted metabolomic analysis of adult *D2hgdh* mutant males. (A) Adult *D2hgdh* mutant males and w^{1118} control males were analyzed using a targeted metabolomic approach. (A) Analysis of the metabolomics data using principal component (PC) analysis. Note that the mutant data group together and are entirely separated from the controls. (B) A heatmap illustrating the top 25 most significantly altered compounds in *D2hgdh* mutants as compared with controls. (C) The relative abundance of lysine in adult *D2hgdh* mutant males and precise a w^{1118} control strain are presented using a box and whiskers plot. Note that lysine levels are either downregulated or unchanged in mutant strains as compared with the control. Figure panels were generated using Metaboanalyst 5.0, as described in the methods. *P*-values calculated using an ANOVA test followed by a Fisher's test to compare mutant samples with control. ***P*<0.01.

SUPPLEMENTAL TABLE

Table S1. Metabolomic analysis of the *D2hgdh* mutants compared with w^{1118} controls. All samples contained 20 adult males. Data are normalized to sample mass and an internal d4-succininc acid standard.

Literature Cited

Achouri, Y., G. Noël, D. Vertommen, M. H. Rider, M. Veiga-Da-Cunha *et al.*, 2004 Identification of a dehydrogenase acting on D-2-hydroxyglutarate. Biochem J 381**:** 35-42.

Adam, J., A. Finch, C. Sepulveda, M. Ducker, M. B. Torroba *et al.*, 2021 Elevated 2HG does not cause features of tumorigenesis. Neuro Oncol 23**:** iv1.

Chou, F. J., Y. Liu, F. Lang and C. Yang, 2021 D-2-Hydroxyglutarate in Glioma Biology. Cells 10.

Chowdhury, R., K. K. Yeoh, Y. M. Tian, L. Hillringhaus, E. A. Bagg *et al.*, 2011 The oncometabolite 2-hydroxyglutarate inhibits histone lysine demethylases. EMBO Rep 12**:** 463-469.

Dang, L., D. W. White, S. Gross, B. D. Bennett, M. A. Bittinger *et al.*, 2009 Cancer-associated IDH1 mutations produce 2-hydroxyglutarate. Nature 462**:** 739-744.

Du, X., and H. Hu, 2021 The Roles of 2-Hydroxyglutarate. Front Cell Dev Biol 9**:** 651317.

Fan, J., X. Teng, L. Liu, K. R. Mattaini, R. E. Looper *et al.*, 2015 Human phosphoglycerate dehydrogenase produces the oncometabolite D-2-hydroxyglutarate. ACS Chem Biol 10**:** 510-516.

Figueroa, M. E., O. Abdel-Wahab, C. Lu, P. S. Ward, J. Patel *et al.*, 2010 Leukemic IDH1 and IDH2 mutations result in a hypermethylation phenotype, disrupt TET2 function, and impair hematopoietic differentiation. Cancer Cell 18**:** 553-567.

Gatto, L., E. Franceschi, A. Tosoni, V. Di Nunno, I. Maggio *et al.*, 2021 IDH Inhibitors and Beyond: The Cornerstone of Targeted Glioma Treatment. Mol Diagn Ther 25**:** 457-473.

Gibson, K. M., H. J. ten Brink, D. S. Schor, R. M. Kok, A. H. Bootsma *et al.*, 1993 Stable-isotope dilution analysis of D- and L-2-hydroxyglutaric acid: application to the detection and prenatal diagnosis of D- and L-2-hydroxyglutaric acidemias. Pediatr Res 34**:** 277-280.

Gramates, L. S., J. Agapite, H. Attrill, B. R. Calvi, M. A. Crosby *et al.*, 2022 FlyBase: a guided tour of highlighted features. Genetics 220.

Gratz, S. J., A. M. Cummings, J. N. Nguyen, D. C. Hamm, L. K. Donohue *et al.*, 2013 Genome engineering of Drosophila with the CRISPR RNA-guided Cas9 nuclease. Genetics 194**:** 1029-1035.

Kranendijk, M., E. A. Struys, G. S. Salomons, M. S. Van der Knaap and C. Jakobs, 2012 Progress in understanding 2-hydroxyglutaric acidurias. J Inherit Metab Dis 35**:** 571-587.

Li, H., G. Chawla, A. J. Hurlburt, M. C. Sterrett, O. Zaslaver *et al.*, 2017 Drosophila larvae synthesize the putative oncometabolite L-2-hydroxyglutarate during normal developmental growth. Proc Natl Acad Sci U S A 114**:** 1353-1358.

Li, H., A. J. Hurlburt and J. M. Tennessen, 2018 A Drosophila model of combined D-2- and L-2-hydroxyglutaric aciduria reveals a mechanism linking mitochondrial citrate export with oncometabolite accumulation. Dis Model Mech 11.

Li, H., and J. M. Tennessen, 2017 Methods for studying the metabolic basis of Drosophila development. Wiley Interdiscip Rev Dev Biol 6.

Li, H., and J. M. Tennessen, 2019 Quantification of D- and L-2-Hydroxyglutarate in Drosophila melanogaster Tissue Samples Using Gas Chromatography-Mass Spectrometry. Methods Mol Biol 1978**:** 155-165.

Losman, J. A., and W. G. Kaelin, Jr., 2013 What a difference a hydroxyl makes: mutant IDH, (R)-2-hydroxyglutarate, and cancer. Genes Dev 27**:** 836-852.

Mahmoudzadeh, N. H., A. J. Fitt, D. B. Schwab, W. E. Martenis, L. M. Nease *et al.*, 2020 The oncometabolite L-2-hydroxyglutarate is a common product of dipteran larval development. Insect Biochem Mol Biol 127**:** 103493.

Mahmoudzadeh, N. H., Y. Heidarian, J. P. Tourigny, A. J. Fitt, K. Beebe *et al.*, 2024 Renal L-2-hydroxyglutarate dehydrogenase activity promotes hypoxia tolerance and mitochondrial metabolism in Drosophila melanogaster. Mol Metab 89**:** 102013.

Nemkov, T., J. A. Reisz, S. Gehrke, K. C. Hansen and A. D'Alessandro, 2019 High-Throughput Metabolomics: Isocratic and Gradient Mass Spectrometry-Based Methods. Methods Mol Biol 1978**:** 13-26.

Öztürk-Çolak, A., S. J. Marygold, G. Antonazzo, H. Attrill, D. Goutte-Gattat *et al.*, 2024 FlyBase: updates to the Drosophila genes and genomes database. Genetics.

Pang, Z., J. Chong, G. Zhou, D. A. de Lima Morais, L. Chang *et al.*, 2021 MetaboAnalyst 5.0: narrowing the gap between raw spectra and functional insights. Nucleic Acids Res 49**:** W388-w396.

Ponomarova, O., H. Zhang, X. Li, S. Nanda, T. B. Leland *et al.*, 2023 A D-2-hydroxyglutarate dehydrogenase mutant reveals a critical role for ketone body metabolism in Caenorhabditis elegans development. PLoS Biol 21**:** e3002057.

Preston, A., K. Reardon, N. Crowson, W. Lamar and J. M. Hirshburg, 2019 D-2-Hydroxyglutaric Aciduria with Enchondromatosis and Angiokeratoma Circumscriptum. Cureus 11**:** e6157.

Reitman, Z. J., S. A. Sinenko, E. P. Spana and H. Yan, 2015 Genetic dissection of leukemia-associated IDH1 and IDH2 mutants and D-2-hydroxyglutarate in Drosophila. Blood 125**:** 336-345.

Sebo, Z. L., H. B. Lee, Y. Peng and Y. Guo, 2014 A simplified and efficient germline-specific CRISPR/Cas9 system for Drosophila genomic engineering. Fly (Austin) 8**:** 52-57.

Struys, E. A., 2006 D-2-Hydroxyglutaric aciduria: unravelling the biochemical pathway and the genetic defect. J Inherit Metab Dis 29**:** 21-29.

Struys, E. A., G. S. Salomons, Y. Achouri, E. Van Schaftingen, S. Grosso *et al.*, 2005a Mutations in the D-2-hydroxyglutarate dehydrogenase gene cause D-2-hydroxyglutaric aciduria. Am J Hum Genet 76**:** 358-360.

Struys, E. A., N. M. Verhoeven, H. J. Ten Brink, W. V. Wickenhagen, K. M. Gibson *et al.*, 2005b Kinetic characterization of human hydroxyacid-oxoacid transhydrogenase: relevance to D-2-hydroxyglutaric and gamma-hydroxybutyric acidurias. J Inherit Metab Dis 28**:** 921-930.

Tian, W., W. Zhang, Y. Wang, R. Jin, Y. Wang *et al.*, 2022 Recent advances of IDH1 mutant inhibitor in cancer therapy. Front Pharmacol 13**:** 982424.

Wang, Y. P., J. T. Li, J. Qu, M. Yin and Q. Y. Lei, 2020 Metabolite sensing and signaling in cancer. J Biol Chem 295**:** 11938-11946.

Yang, Q., J. Hao, M. Chi, Y. Wang, J. Li *et al.*, 2022 D2HGDH-mediated D2HG catabolism enhances the anti-tumor activities of CAR-T cells in an immunosuppressive microenvironment. Mol Ther 30**:** 1188-1200.

Yang, R. R., Z. F. Shi, Z. Y. Zhang, A. K. Chan, A. Aibaidula *et al.*, 2020 IDH mutant lower grade (WHO Grades II/III) astrocytomas can be stratified for risk by CDKN2A, CDK4 and PDGFRA copy number alterations. Brain Pathol 30**:** 541-553.

504 Ye, D., K. L. Guan and Y. Xiong, 2018 Metabolism, Activity, and Targeting of D- and L-2-
505 Hydroxyglutarates. Trends Cancer 4**:** 151-165.
506

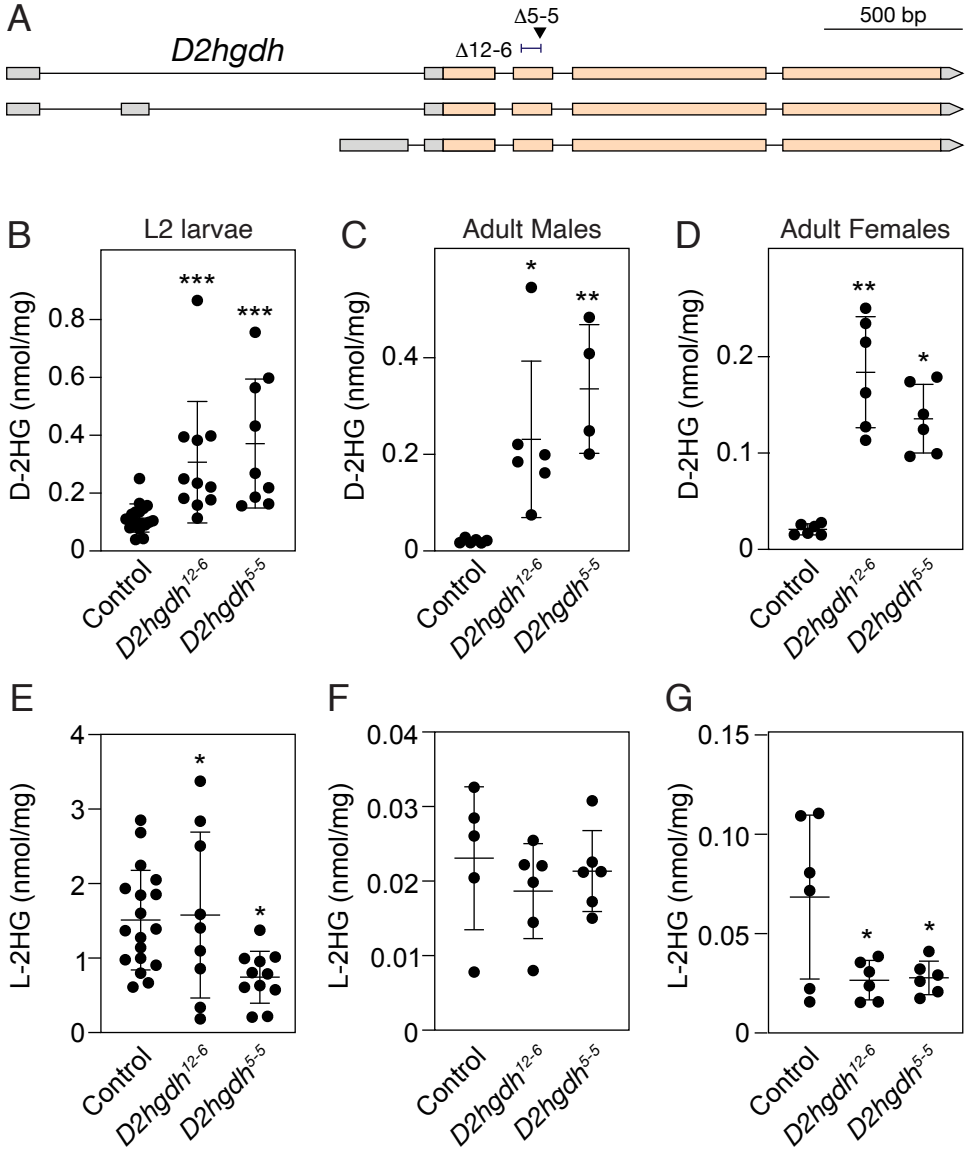

Figure 1

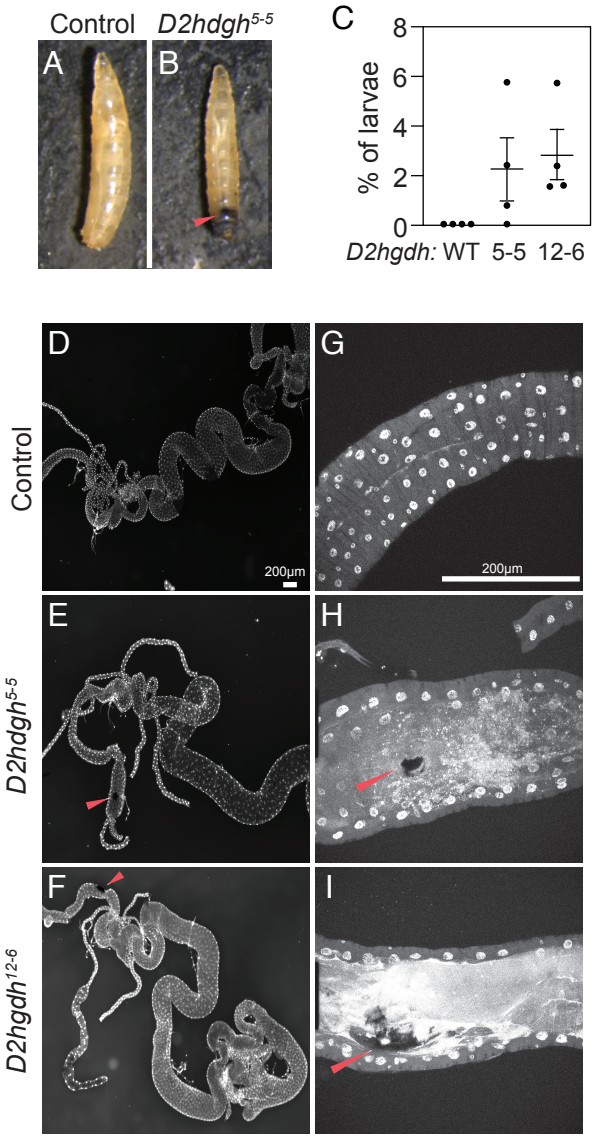

Figure 2

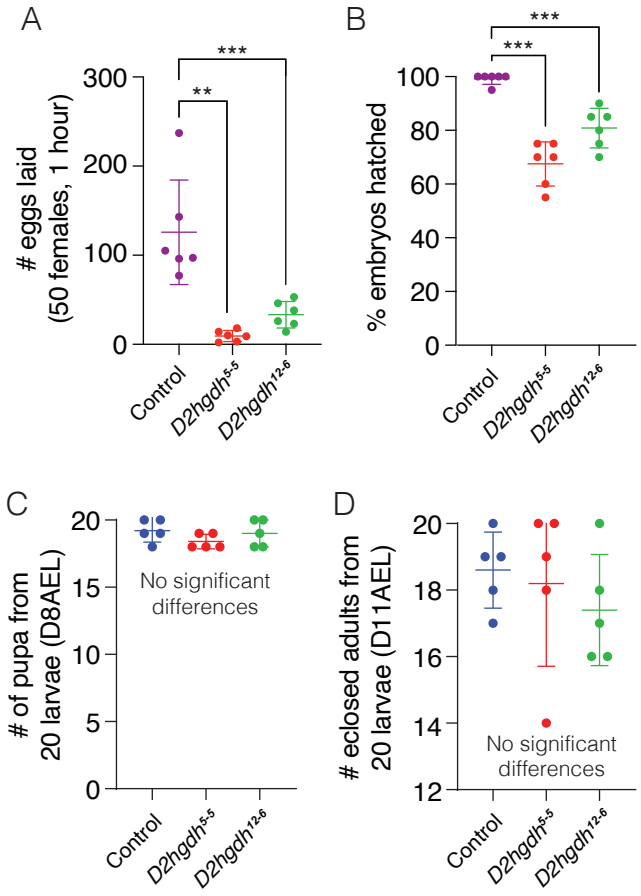

Figure 3

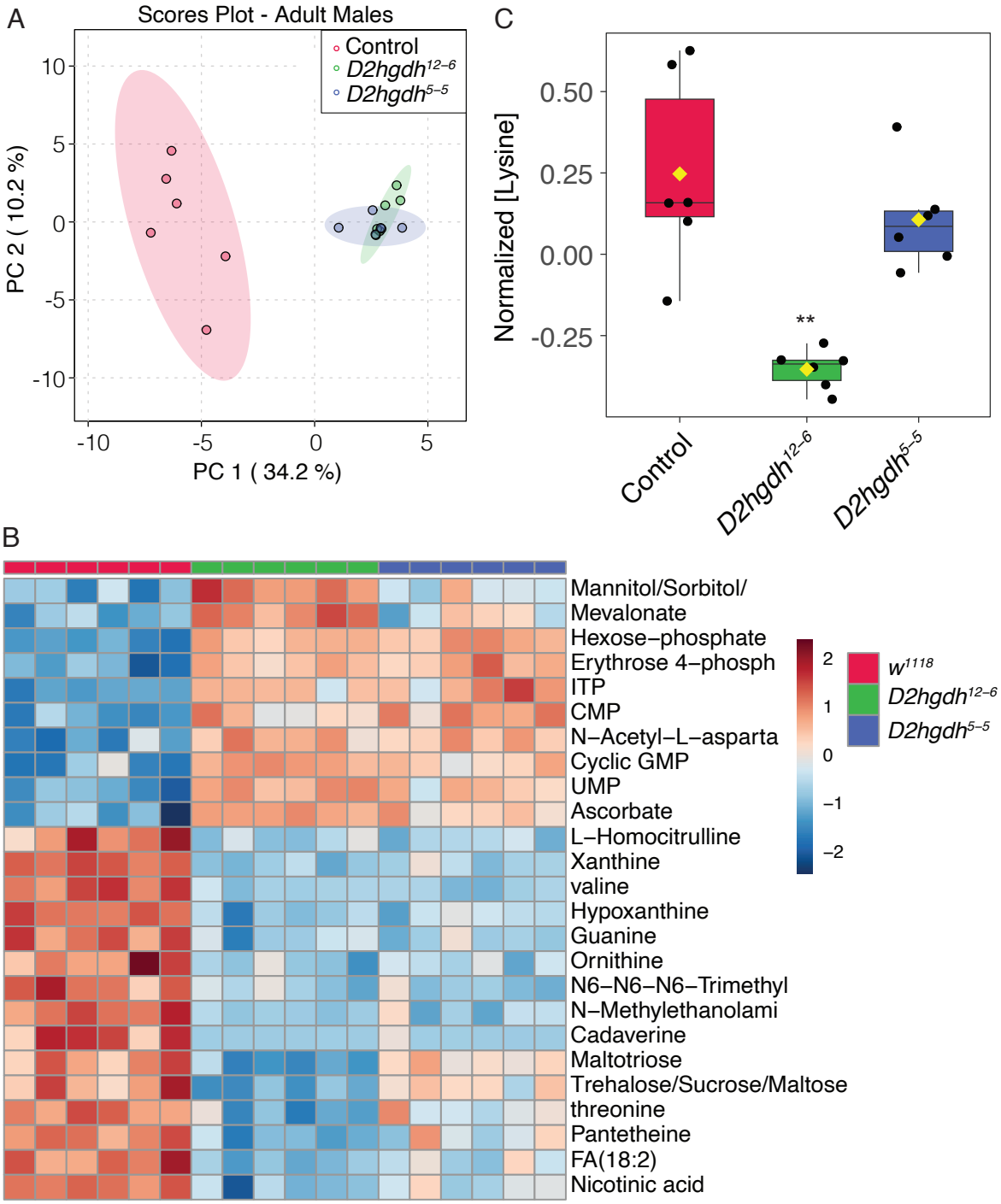

Figure 4